Mechanobiology in Medicine 2 (2024) 100062

Contents lists available at ScienceDirect

Mechanobiology in Medicine

journal homepage: www.sciencedirect.com/journal/mechanobiology-in-medicine

Full Length Article

Extracellular matrix stiffness modulates the mechanophenotypes and focal adhesions of colon cancer cells leading to their invasions via YAP1

Kaide Xia [a,b,f], Wenhui Hu [a,b], Yun Wang [a,b], Jin Chen [a,b], Zuquan Hu [a,b,d,e], Chenyi An [a,b], Pu Xu [a,b], Lijing Teng [a,b], Jieheng Wu [a], Lina Liu [a,b], Sichao Zhang [a,b], Jinhua Long [a,c,**], Zhu Zeng [a,b,d,e,*]

[a] School of Basic Medical Sciences/School of Biology & Engineering, Guizhou Medical University, Guiyang, 550025, PR China
[b] Key Laboratory of Infectious Immunity and Antibody Engineering in Guizhou Province/Engineering Center of Cellular Immunotherapy in Guizhou Province, Guiyang, 550025, PR China
[c] Department of Head & Neck, Affiliated Tumor Hospital of Guizhou Medical University, Guiyang, 550004, PR China
[d] Key Laboratory of Endemic and Ethnic Diseases, Ministry of Education, Guizhou Medical University, Guiyang 550004, Guizhou, PR China
[e] State Key Laboratory of Functions & Applications of Medicinal Plants, Guizhou Medical University, Guiyang, 550004, PR China
[f] Department of Eugenic Genetics, Clinical College of Maternal and Child Health Care, Guizhou Medical University, Guiyang, 550003, PR China

ARTICLE INFO

Keywords:
ECM stiffness
Colon cancer
Mechanophenotypes
Focal adhesions
Metastasis

ABSTRACT

Distal metastasis is the main cause of clinical treatment failure in patients with colon cancer. It is now known that the invasion and metastasis of cancer cells is precisely regulated by chemical and physical factors *in vivo*. However, the role of extracellular matrix (ECM) stiffness in colon cancer cell (CCCs) invasion and metastasis remains unclear. Here, bioinformatical analysis suggested that a high expression level of yes associated protein 1 (YAP1) was significantly associated with metastasis and poor prognosis in colon cancer patients. We further investigated the effects of polyacrylamide hydrogels with different stiffnesses (3, 20, and 38 kPa), which were simulated as ECM, on the mechanophenotype (F-actin cytoskeleton organization, electrophoretic rate, membrane fluidity, and Young's modulus) of CCCs. The results showed that a stiffer ECM could induce the maturation of focal adhesions and formation of stress fibers in CCCs, regulate their mechanophenotypes, and promote cell motility. We also demonstrated that the expression levels of YAP1 and paxillin were positively correlated in patients with colon cancer. YAP1 knockdown reduces paxillin clustering and cell motility and alters the cellular mechanophenotypes of CCCs. This is of great significance for an in-depth understanding of the invasion and metastatic mechanisms of colon cancer and for the optimization of clinical therapy from the perspective of mechanobiology.

1. Introduction

Colon cancer is one of the most common malignant tumors and ranks second in terms of cancer-related deaths worldwide.[1,2] However, distant metastasis is considered the primary cause of clinical treatment failure in patients with colon cancer,[3–5] with an overall 5-year survival rate accounting for only 13.3%.[6] Our bioinformatics analyses found that the higher expression levels of yes associated protein 1 (YAP1), which is a core transcriptional coactivator and transducer of mechanical stimuli in patients with colon cancer, were associated with their metastasis and poor prognoses. Physical and chemical factors in the solid tumor microenvironment are key to regulating the occurrence and development of cancer cells.[7,8] An increasing number of researchers have focused on the mechanochemical coupling mechanism of the effects of increased extracellular matrix (ECM) stiffness, blood flow/interstitial flow shear stress, and static pressure on tumor cell proliferation and metastasis.[9,10] ECM stiffness plays an important role in the regulation of cancer cell migration and invasion.[11,12] Cells can sense and respond to various extracellular mechanical stimuli to ensure proper physiological functions, such as adhesion, migration, invasion, and progression of various diseases, including cancer.[13,14] Extracellular mechanical signals are transmitted by activating intracellular signaling pathways via mechanical sensors in the cell plasma membrane.[15,16] The force applied to ECM-integrin adhesion can activate focal adhesion kinase (FAK) and

* Corresponding author. School of Basic Medical Sciences/School of Biology & Engineering, Guizhou Medical University, Guiyang, 550025, PR China.
** Corresponding author. Department of Head & Neck, Affiliated Tumor Hospital of Guizhou Medical University, Guiyang, 550004, PR China.
E-mail addresses: longjinhua100@sina.cn (J. Long), zengzhu@gmc.edu.cn (Z. Zeng).

https://doi.org/10.1016/j.mbm.2024.100062
Received 23 September 2023; Received in revised form 10 March 2024; Accepted 13 March 2024
Available online 19 March 2024

promote the formation of focal adhesions (FAs), thereby recruiting adhesion-related proteins (e.g., vinculin, talin, and paxillin) to trigger downstream signaling cascades.[17] FAs are dynamic multi-protein complexes that participate in ECM adhesion and play an important role in translating ECM stiffness signals into intracellular chemical responses. The dynamic cycle of FAs assembly and disassembly at the edge of a migrating cell provides a directional force for movement; FAs dysfunction is an important step in tumor cell invasion and metastasis.[18] Therefore, it can be hypothesized that colon cancer cells (CCCs) sense and respond to changes in ECM stiffness via YAP1 and FAs, leading to invasion and metastasis.

To verify this hypothesis, we used a polyacrylamide (PA) hydrogel to simulate the stiffness microenvironment of normal colon tissue and colon cancer tissue under physiological and pathophysiological conditions and investigated the effects of different ECM stiffnesses on the mechano-phenotypes, including morphology, adhesion, invasion, electrophoresis rate, membrane fluidity, and Young's modulus of CCCs. In addition, we explored the molecular mechanisms by which ECM stiffness regulates the migration and invasion of colon cancer cells. Therefore, it is important to understand the mechanism of CCCs metastasis from the perspective of mechanobiology to optimize and personalize clinical treatment strategies for patients.

2. Material and methods

2.1. Bioinformatic analysis

The UALCAN database (https://ualcan.path.uab.edu)[19] was used to analyze the mRNA levels of YAP1 genes in pan-cancer based on The Cancer Genome Atlas (TCGA) database. In this study, we used this database to analyze the expression of YAP1 in colon cancer and normal tissues, as well as node metastasis status. The Gene Expression Omnibus (GEO) database (https://www.ncbi.nlm.nih.gov/geo/) was used to analyze the expression levels of YAP1 in colon cancer (GSE 39582) based on distant metastasis status, and patients were subgrouped into no distant metastasis (M0) and distant metastasis (M1) groups. GEPIA (http://gepia.cancer-pku.cn)[20] was used to analyze the correlation between the expression of YAP1 and paxillin in colon adenocarcinoma from TCGA database. The Human Protein Atlas (HPA) database (www.proteinatlas.org) was used to analyze the protein levels of YAP1 in colon normal and cancer tissues by immunohistochemical (IHC) staining.

2.2. Cell culture

The CCCs (HCT116) were donated by the Institute of Oncology, Affiliated Tumor Hospital of Guangzhou Medical University (Guangzhou, China). This protocol was approved by the Human and Animal Ethics Committee of Guizhou Medical University (No. 2023-46). The cells were cultured in RPMI-1640 medium (Gibco) containing 10% fetal bovine serum (Biological Industries) and 1% antibiotics (streptomycin and penicillin, Gibco). Cells were incubated in a humidified incubator at 37 °C containing 5% CO_2. The cells were harvested using trypsin-EDTA (Gibco) and cultured on hydrogel substrates for further experiments.

2.3. Preparation of polyacrylamide hydrogel

PA hydrogels of different stiffnesses were prepared according to the protocols of Tse[21] and Peng.[22] Briefly, 40% acrylamide (Aladdin) and 2% bis-acrylamide (Sigma-Aldrich) were mixed in varying proportions, and then 10% ammonium persulfate (APS, Aladdin) and 0.1% tetramethylethylenediamine (TEMED, Sigma-Aldrich) were gently mixed and added to a hydrogel mold, which was polymerized at room temperature for 20 min to obtain a final thickness of 0.75 mm. The surface of the hydrogel substrate was applied with 0.2 mg/ml sulfosuccinimidyl-6-(4′-azido-2′-nitrophenylamino)-hexanoate (Sulfo--SANPAH, Thermo-Fisher Scientific) under 365 nm ultraviolet (UV) light for 25 min. These hydrogels were coated with collagen I (0.25 mg/ml) in phosphate-buffered saline (PBS) and incubated overnight at 4 °C. The following day, the collagen I solution was removed from the hydrogel, which were then kept in PBS at 4 °C until cell culture.

2.4. Rheological testing

A rheometer was used to determine the Young's modulus of the PA hydrogels. The detection method and calculation of the Young's modulus were based on the work published by Sana et al.[23] Before measurement, the hydrogels were immersed in deionized water to remove non-crosslinked monomers, swollen to an equilibrium state at room temperature for 24 h, and then split into small round pieces with a diameter of 20 mm. Storage modulus (G′) was measured by modular compact rheometer (Anton Paar, Germany) with a 20 mm upper parallel plate geometry, oscillatory frequency sweep test from 1 to 10 Hz, and a constant 2% strain. Young's modulus was calculated using the following equation:

$$E = G' 2(1 + v) \quad (1)$$

where E is Young's modulus, G′ is storage modulus and v is the Poisson's ratio (0.5 for PA hydrogel).

2.5. Cell morphology

HCT116 cells were cultured on PA hydrogels at a density of 1×10^4 cells/well. After 24, 48, and 72 h, cells were photographed under an inverted microscope. Cell morphology (cell area, circularity, and aspect ratio) was analyzed using ImageJ software.

2.6. Spheroid spreading assay

The spheroid spreading assay was performed as described previously.[24,25] In brief, the wells of a 96-well-plate were coated with 50 μl of 1% agarose (Millipore Sigma) in PBS, then seeded with 100 μl of the cell suspension (3×10^3 cells). Multicellular spheroids were obtained after culturing for 4 days. Then, the spheroids were collected and inoculated on cell culture plates with PA hydrogels, and images were captured at 4 and 24 h time points using an inverted microscope. Finally, to quantify the degree of dispersion, images were analyzed using ImageJ software to outline the periphery of the aggregate, and the total area of the 24 h image was divided by the area of the initial image.

2.7. Time-lapse imaging

For free migration experiments, the cells were seeded onto the PA hydrogel for 12 h. The complete medium was replaced with medium containing 1% serum. Subsequently, the live cell workstation was debugged and real-time photo parameters were set to capture images every 10 min using a 10× objective lens. The recording lasted for 9 h. The acquired images were used to generate cell trajectories using the ImageJ software. In addition, the DiPer open-source program was used to calculate the cell trajectory, average cell velocity, and mean azimuth movement.[26]

2.8. Atomic force microscopy (AFM)

The Young's modulus of the cells were measured using atomic force microscopy (AFM; JPK NanoRacer, Bruker). Cells were inoculated onto hydrogels of different stiffness and cultured for 48 h. Subsequently, the medium was aspirated and the cells were washed twice with PBS. The probe was then subjected to detection at a constant velocity of 2.0 μm/s, while experiencing a force ranging from 0.1 to 1 nN. Standard silicon nitride cantilever with an elastic coefficient of 0.03 N/m was employed. The probe itself possessed an elastic coefficient of 0.08 N/m, a spherical

needle measuring 10 μm, and a Poisson's ratio of 0.5. The experiment was carried out under controlled conditions, specifically in a quiet and clean environment with a constant temperature of 25 °C. Forty cells were randomly selected from each sample and each cell was measured twice. Following the acquisition of force and distance curves, the JPK image processing software was utilized to fit and analyze the curves within the range of 0–200 pN in the needle loading curve. Subsequently, Young's modulus of the cells were determined based on the fitting curves.

2.9. Electrophoretic mobility (EPM)

The measurement technique employed for the EPM was outlined in a previous study.[27] In brief, cells were cultured on hydrogels of different stiffness for 48 h. Subsequently, the cells were digested using trypsin-EDTA, harvested, and fixed with 1% glutaraldehyde at room temperature for 10 min. The resulting cell suspension was prepared at a concentration of 5×10^5 cells/ml using 9% (w/v) sucrose solution. The cell suspension was then injected into a cell electrophoretic migration chamber, which was mounted onto a microscope platform. During the examination using a low-power microscope, it was determined that the static layer occupied 1/10 of the distance between the front and back wall lines. Consequently, the experimental measurements were conducted within the static layer. Each group selected 20 cells and recorded the time it took for these cells to traverse two cells, with each cell measuring 50 μm. The measurements were conducted at a temperature of 25 °C and a voltage of 50 V. The average time for 20 cells was calculated and the electrophoresis rate of the cells was determined.

2.10. Cell membrane fluidity

Cells were cultured on hydrogels of different stiffness for 48 h. After washing twice with PBS, they were treated with a 1 ml solution of the DPH probe, ensuring that light sources were avoided, and the cells were subsequently incubated at a temperature of 37 °C for a period of 30 min. Following two washes with PBS, trypsin digestion was performed, followed by washing with PBS, and finally collection. The cell count was determined and the cells were suspended in 1 ml of PBS, resulting in a cell concentration of 1×10^6 cells/ml. The fluorescence intensity (I) of cells at various polarization angles was measured using a time scan on a fluorescence spectrometer. The excitation wavelength (λ EX) was set to 360 nm, the emission wavelength (λ EM) to 430 nm, and the emission slit to 5 nm. The scanning process lasted 10 s, and each sample was scanned three times. The labeled cells were measured within a maximum time frame of 2 h, ensuring cell viability throughout the measurement procedure. The calculation of fluorescence polarization (P) is determined by the formula: $P=(I_{VV}\text{-}GI_{VH})/(I_{VV} + GI_{VH})$, whereby the P value exhibits an inverse relationship with the fluidity of cell membrane.

2.11. Immunofluorescence of focal adhesion

The cells were cultured on hydrogels of different stiffness for 48 h and fixed with 4% paraformaldehyde for 15 min. The cells were permeabilized with 0.5% Triton X-100 for 5 min. The cells were then washed with PBS and blocked with a 1% BSA solution for 60 min. The cells were incubated with primary antibodies (1:100), including anti-Paxilin (Abcam), anti-Talin (Abcam), and anti-Vinculin (Abcam) overnight at 4 °C. After the cells were washed thrice with PBS and incubated with a secondary goat anti-rabbit IgG (1 : 200) (Abcam), nuclear counterstaining was performed using DAPI. Finally, the fluorescence was observed and photographed using a laser confocal microscope.

2.12. YAP1 knockdown of CCCs

YAP1-shRNA and shNC lentiviruses were purchased from Shanghai GENECHEM Company. Lentiviral infection was performed according to the manufacturer's protocol. Briefly, CCCs were seeded in 6-well cell

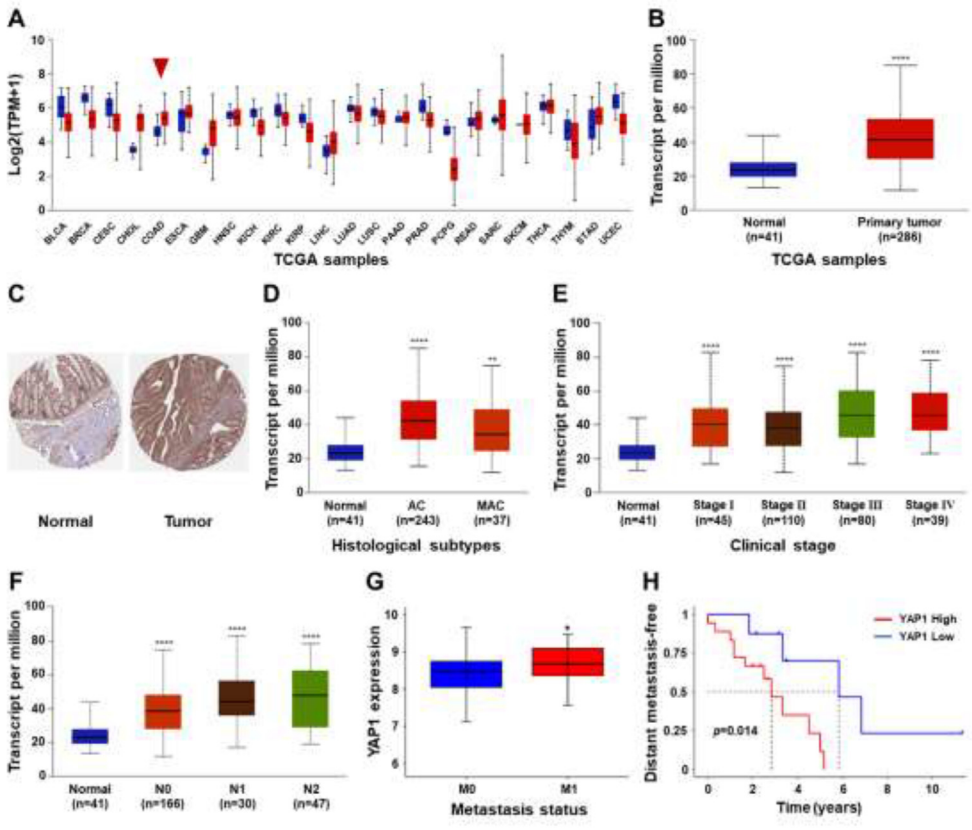

Fig. 1. YAP1 expression was associated with metastasis and poor prognosis in colon cancer (A) Pan-cancer. expression of YAP1 in human cancers from TCGA database. Colon adenocarcinoma (COAD) highlighted with a red arrowhead. (B) Expression of YAP1 in normal colon tissues and colon adenocarcinoma tissues from TCGA database. (C) Immunohistochemical analysis of YAP1 protein expression in normal colon tissues and colon adenocarcinoma tissues from Human Protein Atlas (HPA) database. (D) Expression of YAP1 in colon adenocarcinoma based on histological subtypes from the TCGA. AC, Adenocarcinoma; MAC, Mucinous adenocarcinoma. (E) Expression of YAP1 in colon adenocarcinoma based on clinical stage from the TCGA. (F) Expression of YAP1 in colon adenocarcinoma based on lymph nodal metastasis status from the TCGA database (N0, No regional lymph node metastasis; N1, Metastases in 1–3 axillary lymph nodes; N2, Metastases in 4–9 axillary lymph nodes; N3, Metastases in 10 or more axillary lymph nodes). (G) Expression of YAP1 in colon cancer tissues with metastasis and without metastasis from the GEO database (M0, no regional or distant metastasis; M1, regional or distant metastasis). (H) Distant metastasis-free survival (DMFS) for colon cancer patients with low (blue line) and high (red line) YAP1 expression from the GEO database. (mean ± SD; $*p < 0.05$, $**p < 0.01$ and $****p < 0.0001$).

culture plates at a density of 3.5×10^5 cells/well and incubated for 12 h. Then, lentivirus-containing cell culture medium was added to the cells. After 8 h, the medium was replaced with fresh medium. After 24 h, the cells were replaced with fresh complete medium and treated with 4 μg/ml puromycin. Finally, the knockdown efficiency was confirmed by qRT-PCR, western blotting, and immunofluorescence in cells, which were used for subsequent experiments. The detailed target sequences were as follows:

Gene name	Sequence
shNC	TTCTCCGAACGTGTCACGT
shYAP1-1	GCTCATTCCTCTCCAGCTTCT
shYAP1-2	GCAGCAGAATATGATGAACTC
shYAP1-3	GCTGCCACCAAGCTAGATAAA

2.13. RNA isolation and quantitative real-time polymerase chain reaction (qRT-PCR)

Total cellular RNA was extracted using Trizol Reagent (Invitrogen) according to the manufacturer's protocol. cDNA was synthesized using a cDNA Reverse Transcription Kit (Thermo Fisher Scientific), and mRNA expression was analyzed by quantitative real-time reverse transcription polymerase chain reaction with SYBR green (Takara). The $2^{-\Delta\Delta Ct}$ method was used to analyze the relative mRNA levels of target gene. GAPDH was used as an internal control. The following primer sequences were used:

Gene name	Sequence
YAP1-forward	AGGAGAGACTGCGGTTGAAA
YAP1-reverse	CCCAGGAGAAGACACTGCAT
GAPDH-forward	GACCTGACCTGCCGTCTA
GAPDH-reverse	AGGAGTGGGTGTCGCTGT

2.14. Western blotting (WB) analysis

Cells were cultured on hydrogels of different stiffnesses in 6-well cell culture plates and lysed on ice for 10 min using RIPA protein lysis buffer (containing PMSF, protease inhibitors, and phosphatase inhibitors). The lysates were collected in 1.5 ml centrifuge tubes and centrifuged at 12000 rpm for 25 min at 4 °C. The supernatants were collected in new prechilled 1.5 ml centrifuge tubes and stored on ice until use. The protein concentration was determined by BCA protein detection kit. Proteins were separated by 10% sodium dodecyl sulfate-polyacrylamide gel electrophoresis and transferred to PVDF membranes (Millipore). The membranes were blocked using 5% BSA at room temperature for 1 h and incubated with specific primary antibodies (1:1000) overnight at 4 °C. After washing with TBST, the corresponding horseradish peroxidase-labeled secondary antibodies (1:5000) were added and incubated at room temperature for 1 h, and the signal was detected using the ECL

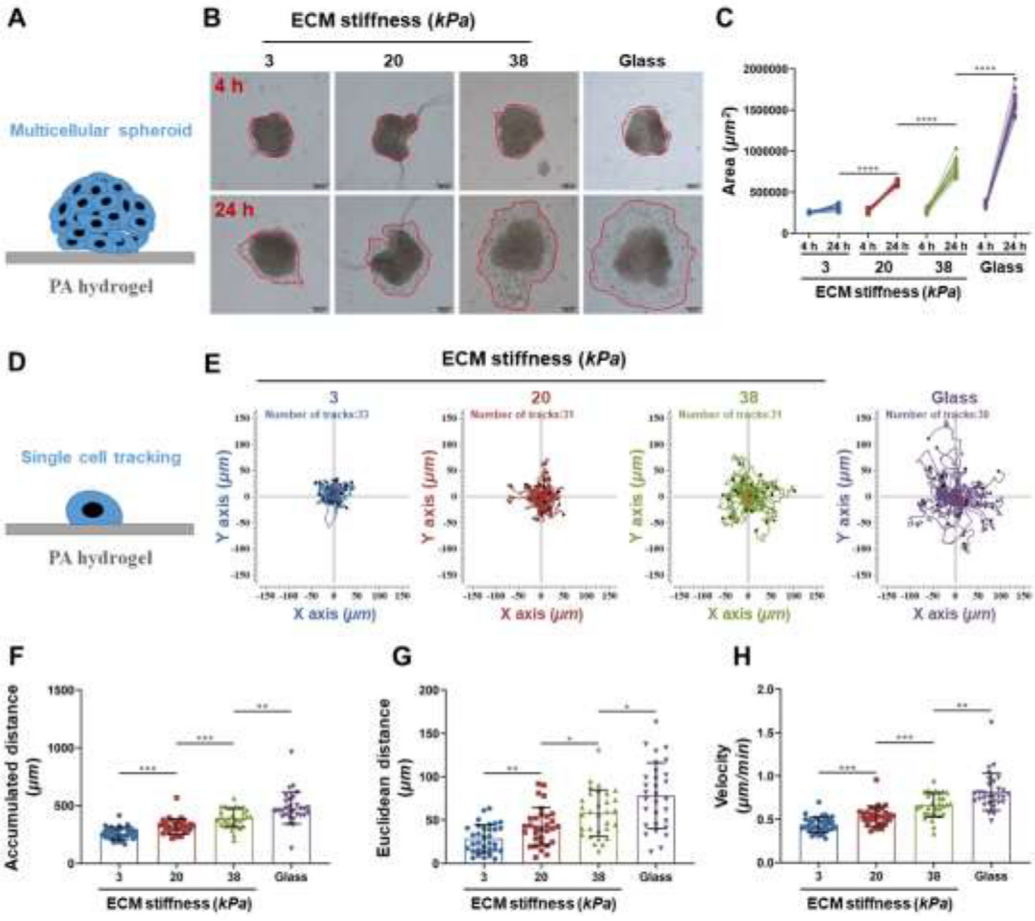

Fig. 2. ECM stiffness increases the invasiveness of cancer cells. (A) and (B) CCCs multicellular spheroids were transferred to hydrogels of different stiffnesses (3, 20, and 38 kPa) and glass, and imaged at 4 and 24 h post-plating. Scale bar = 200 μm. (C) ImageJ software was used to calculate the area of each spheroid at 4 h and 24 h by manually outlining the spheroids at the indicated time points. (D) and (E) CCCs were cultured on hydrogels of different stiffness for 12 h and immediately recorded by time-lapse microscopy for 9 h, and trajectories of the cells were plotted for 9 h. (F–H) Accumulated distance, Euclidean distance and average velocity were calculated and analyzed with DiPer software. (mean ± SD, $*p < 0.05$, $**p < 0.005$, $***p < 0.0005$ and $****p < 0.0001$).

method. GAPDH was selected as the internal reference and ImageJ software was used for gray value analysis.

2.15. Statistical analysis

Data are presented as mean ± standard deviation (SD). Comparisons between two groups were performed using the unpaired t-test, and comparisons between three or more groups were performed using one-way ANOVA. *P* values for statistical significance are represented as ns $p > 0.05$, *$p < 0.05$, **$p < 0.01$, ***$p < 0.001$, and ****$p < 0.0001$.

3. Results

3.1. Higher YAP1 expression levels in colon cancer were associated with their metastasis and poor prognosis

Various extracellular mechanical factors regulate cancer development and progression. YAP1 is an important mechanotransducer that senses mechanical stimuli[28] and translates signals to control transcriptional programs by translocating to the nucleus.[29] To explore the role of YAP1 in the progression and metastasis of colon cancer, we first analyzed the expression of YAP1 in pan-cancer cells using the UALCAN online tool to obtain RNA-seq data from TCGA database. As shown in Fig. 1 A and B, the mRNA expression level of YAP1 was significantly elevated in colon cancer tissues compared to normal controls. We also analyzed the YAP1 protein levels using immunohistochemical staining data from the HPA database. Compared to normal colon tissues, the protein expression level of YAP1 was significantly upregulated in colon cancer tissues (Fig. 1C), which was consistent with the corresponding mRNA levels. The relationship between the expression of YAP1 and patient clinicopathological variables along histological subtypes (Fig. 1D) and clinical stage (Fig. 1E) was investigated. As shown in Fig. 1F, the expression level of YAP1 in patients with lymph node metastasis (N1–3) was significantly higher than that in patients without lymph node metastasis (N0). In addition, the GSE database used to analyze YAP1 expression levels in colon cancer patients with or without distant metastasis (Fig. 1G) demonstrated that the expression of YAP1 was significantly enhanced in patients with distant metastasis compared to patients without distant metastasis. Finally, the correlation between YAP1 expression and distant metastasis-free survival (DMFS) in colon cancer patients revealed that the DMFS of patients with high YAP1 expression was significantly lower than that of patients with low YAP1 expression (Fig. 1H). These results demonstrate that altered expression levels of YAP1 affect cancer metastasis and reduce patient survival rates in the development and progression of colon cancer.

3.2. ECM stiffness enhanced CCCs' invasion

Studies have shown that ECM stiffness in tumor tissues is closely associated with malignant transformation and cancer.[30–32] To investigate the effects of ECM stiffness on the migration and invasion capacities of colon cancer cells, we prepared PA hydrogels with adjustable stiffness through oxidation-reduction radical polymerization by changing the concentration ratio of acrylamide and bis-acrylamide, APS initiator, and TEMED catalyst (Fig. S1A). The Young's modulus of the PA hydrogels were measured using a rheometer, as shown in Figure S1 C. A soft hydrogel of 3 kPa was used to simulate normal colon tissue,[33] while 20 kPa and 38 kPa hydrogels

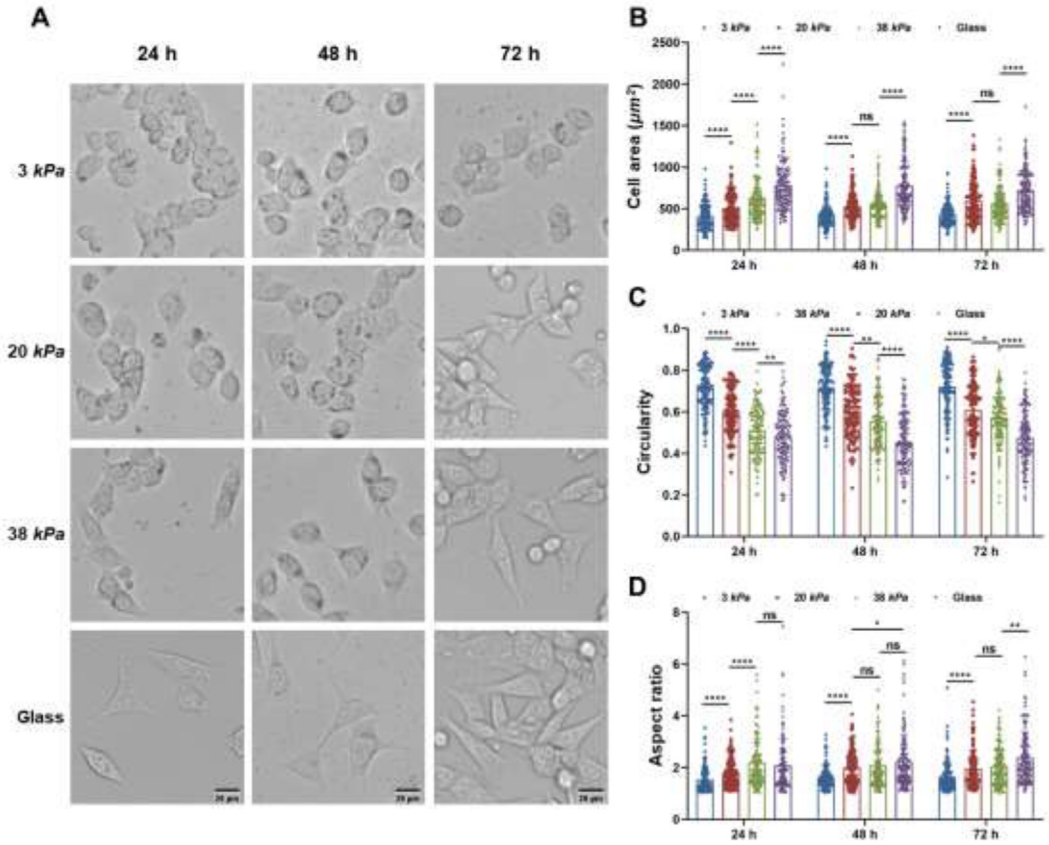

Fig. 3. Time-dependent morphological changes of cell on different ECM stiffness. (A) Representative phase-contrast images of CCCs cultured on hydrogels of different stiffness for 24, 48, and 72 h, cell morphology and spreading were observed by an inverted microscope. Scale bar = 20 μm. (B) Spread area. (C) Circularity. (D) Aspect ratio. Cell morphology was analyzed using ImageJ software. (mean ± SD, *$p < 0.05$, **$p < 0.01$, ***$p < 0.001$ and ****$p < 0.0001$).

were used to simulate the ECM stiffness of malignant colon cancer tissues.[34] Meanwhile, the cytotoxicities of PA hydrogels to CCCs were detected by the CCK8 method, and the results showed that PA hydrogels were not cytotoxic to CCCs (Figs. S2 and S3), making them suitable for subsequent experiments.

CCCs (HCT116) were cultured into multicellular spheres, which were then inoculated on PA hydrogels of different stiffnesses, and cell adhesion and invasiveness after 4 and 24 h (Fig. 2A and B). After 24 h of sphere culture, the spheres cultured on the 3 kPa soft hydrogel remained spherical with clear edges, a small number of single cells around the spheres invaded the surrounding environment, and the cells in the invaded environment showed a round shape (Fig. 2B). The cell spheres cultured on stiffer hydrogels (20 and 38 kPa) had larger adhesion areas and higher degrees of invasion than those cultured on soft hydrogels (Fig. 2B and C). These data suggest that a stiffer ECM promotes the aggressiveness of CCCs, further proving that ECM stiffness in the tumor microenvironment could be involved in the regulation of tumor cell metastasis. Single-cell tracking analysis showed (Fig. 2E–H) that the motility of CCCs was weakest on the soft hydrogel at 3 kPa. Compared to the cells on the soft hydrogel, the Accumulated distance (Fig. 2F), Euclidean distance (Fig. 2G) and cell movement velocity (Fig. 2H) significantly increased along with enhanced ECM stiffness. Taken together, these results indicate that CCC motility was regulated by ECM stiffness.

3.3. ECM stiffness facilitated CCCs' polarization during migration

The first step of cell invasion is the polarization and formation of the front-rear polarity axis, which controls orientation and persistence during cell migration.[35] Morphological changes in CCCs cultured on PA hydrogels with different stiffnesses (3, 20, and 38 kPa) at 24, 48, and 72 h were observed using an inverted microscope. As shown in Fig. 3 A and B, the cells on the stiffer hydrogels (20 and 38 kPa) gradually became spindle and irregular in shape, and the spreading areas of the cells also increased. In contrast, the volume of cells cultured on the soft hydrogel (3 kPa) decreased, with a low cell spreading area and a round shape. However, cells cultured on the 20 and 38 kPa hydrogels showed no significant difference in cell area between 48 and 72 h. The roundness (Fig. 3C) and aspect ratio (Fig. 3D) of the cells significantly decreased and increased, respectively, along with an enhanced hydrogel stiffness. Thus, ECM stiffness facilitates cell polarization during migration.

3.4. ECM stiffness tuned mechanophenotypes of CCCs into invasive phenotypes

Mechanophenotypes of cells reflect the relationship between their structure and function. To investigate the effects of ECM stiffness on CCC mechanophenotypes, first, the Young's modulus of cells cultured on hydrogels with different stiffnesses were measured by AFM, as shown in

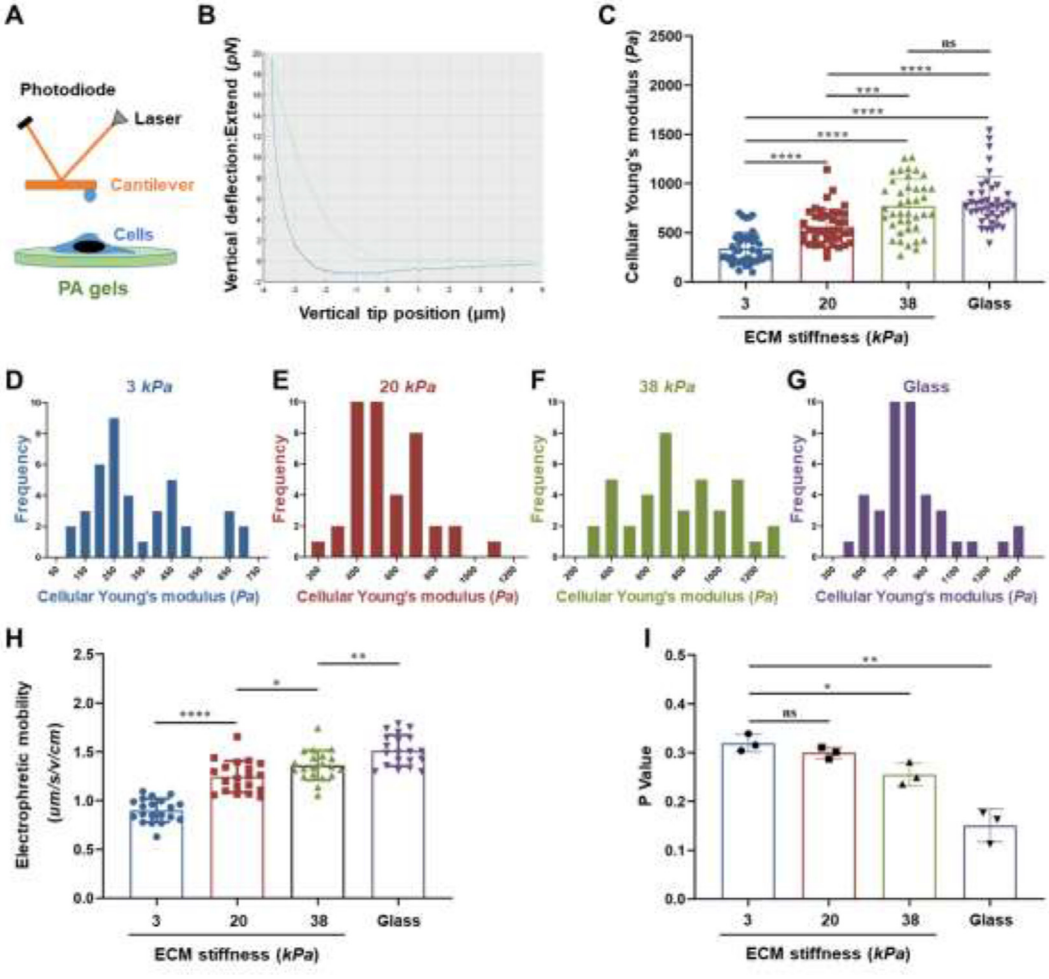

Fig. 4. ECM stiffness affected the cellular biomechanical properties of CCCs. (A) Illustration of AFM measurement technique: an individual adherent CCC was measured with 10 μm bead carrying cantilever. (B) Force-distance curves were analyzed by JPK software. (C) The average Young's modulus of CCCs cultured on hydrogels of different stiffness, detected by AFM. (D–G) The Young's modulus distribution of CCCs cultured on hydrogels of different stiffness. (H) The electrophoretic mobility of CCCs cultured on hydrogels of different stiffness. (I) The fluorescence polarization parameter of CCCs cultured on hydrogels of different stiffness. (mean ± SD; $*p < 0.05$, $**p < 0.01$ and $****p < 0.0001$).

Fig. 4C. The Young's modulus of cells increased with hydrogel stiffness (3, 20, and 38 kPa), but there was no significant difference between the 38 kPa and glass groups (Fig. 4D–G). Second, the EPM reflects the amount of negative charge carried by the plasma membrane. As shown in Fig. 4H, EPM increased significantly along with increase in hydrogel stiffness, indicating that the repulsive forces between the CCCs increased. Third, the membrane fluidity of CCCs was quantified using the fluorescence polarization parameter (p), which was negatively correlated with the motility of membrane lipid molecules. The results showed that the p value decreased with increasing hydrogel stiffness, indicating that the motility of the membrane lipid molecules of the cells significantly increased (Fig. 4I). No significant differences were observed between 3 and 20 kPa. These results demonstrate that the mechanophenotypes of CCCs are regulated by ECM stiffness, which promotes their invasive phenotypes.

3.5. Paxillin clustering in CCCs contributed to F-actin reorganization in stiffness-dependent manner

During cell migration, the dynamic cycle of FA assembly and disassembly at the edge of a migrating cell provides a traction force, the dysfunction of FAs is an important step in tumor cell invasion and metastasis.[18,36] Thus, we hypothesized that ECM stiffness promotes CCC migration via abnormal FAs dynamics. First, the expression levels of adhesion-associated proteins (paxillin, talin, and vinculin) and formation of FAs in CCCs cultured on hydrogels of various stiffnesses were investigated using immunofluorescence. The results showed (Fig. S4) that paxillin could be involved in the regulation of FAs formation in CCCs. Therefore, paxillin was used as the FA marker. As shown in Fig. 5A, paxillin was diffusely distributed in the cytoplasm of cells grown on the 3

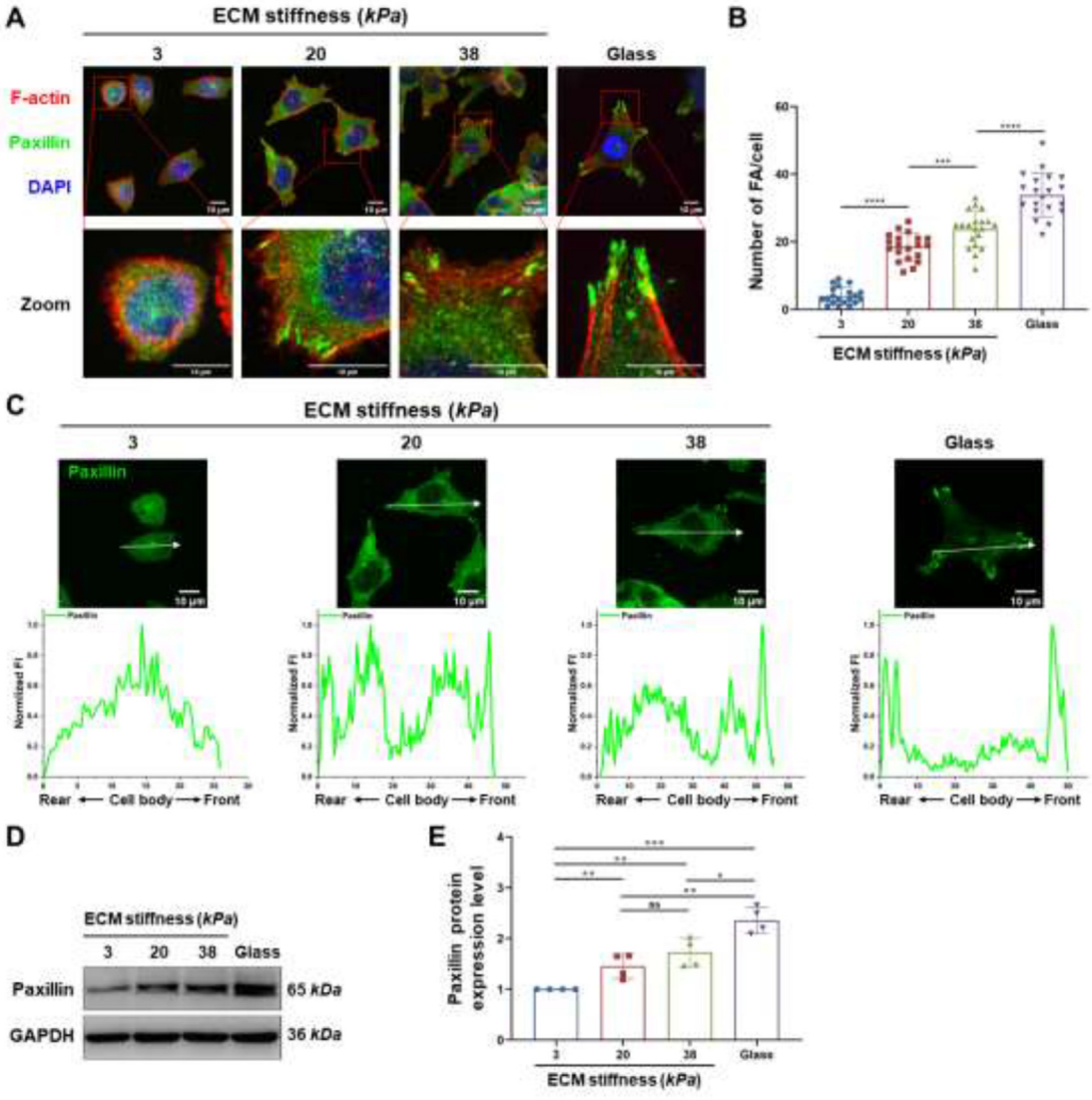

Fig. 5. Stiff ECM promoted focal adhesion formation. (A) CCCs were inoculated on hydrogels of different stiffness for 48 h, and then focal adhesions formation was examined by paxillin immunostaining (green). Nuclei were stained with DAPI (blue), and actin cytoskeleton was stained with phalloidin (red). Red boxes show the region of interest that is magnified. Scale bar = 10 μm. (B) Quantification of FA numbers. (C) Representative immunofluorescence images stained with anti-paxillin antibody (green) in CCCs. The intensity distribution of paxillin (green) along the direction of the white arrowhead shown in the line scan plot. (D, E) The expression levels of paxillin on hydrogels of different stiffness were detected by western blotting and the relative quantification. (mean ± SD, $*p < 0.05$, $**p < 0.01$, $***p < 0.001$ and $****p < 0.0001$).

kPa hydrogel. However, in cells cultured on stiff hydrogels (20 and 38 kPa), paxillin was distributed in dense clusters and accumulated specifically at the ends of fasciculate actin microfilaments. Moreover, CCCs cultured on stiffer hydrogels (Fig. 5A) typically formed polarized stress fiber bundles compared with those cultured on soft hydrogels, and the number of paxillin clusters per cell increased in a hydrogel stiffness-dependent manner (Fig. 5B). The distribution of paxillin in the front-rear polarity axis of the cells was analyzed, and the results (Fig. 5C) showed that paxillin in cells cultured on a soft substrate (3 kPa) was progressively distributed from the edge to the center. With increasing hydrogel stiffness, paxillin is transferred from the center to the edge, leading to FAs formation. In addition, the protein expression levels of paxillin were significantly upregulated in the stiffer hydrogels (Fig. 5D and E). These results indicated that ECM stiffness promotes the formation of FAs at the anterior membrane prominence of CCCs, suggesting that paxillin clusters are involved in cell polarization.

3.6. *ECM stiffness regulated the motility and morphology of CCCs via YAP1 signaling pathway*

It is well known that YAP1 is a type of mechanosensitive transcription factor in cells. As shown in Fig. 6A, B, and C, the mRNA and protein expression levels of YAP1 in CCCs cultured on stiffer hydrogels were significantly upregulated. Moreover, the localization of YAP1 was measured by immunofluorescence staining (Fig. 6D) and nuclear-cytoplasmic protein separation by WB (Fig. S5); the results showed that the fluorescence intensities of YAP1 in the cytoplasm of CCCs cultured on soft hydrogels (3 kPa) and stiffer hydrogels (20 and 38 kPa) were significantly stronger and weaker, respectively, than those in the nucleus, while the expression levels of phosphorylated YAP1 (p-YAP1) in the cytoplasm of CCCs cultured on soft hydrogels were significantly higher than those of stiffer hydrogels, indicating that CCCs could respond to changes in ECM stiffness via the YAP1 signaling pathway. To further explore the potential mechanisms of YAP1 in CCCs in response to changes in ECM stiffness, the expression of YAP1 in CCCs was inhibited using the YAP1 inhibitor verteporfin (VP) and short hairpin RNA (shRNA). As shown in Figures S6 and S7, the YAP1 expression in CCCs and cells invasion were effectively inhibited by 1 μM VP and shYAP1-3. Therefore, 1 μM VP and shYAP1-3 were chosen for subsequent experiments. As shown in Fig. 7, multicellular spheroids cultured on stiffer hydrogels (20 and 38 kPa) treated with VP (Fig. 7A and B) and shYAP1 (Fig. 7C and D) showed decreased overall motility (Fig. 7E and F). These results demonstrate that YAP1 is involved in the regulation of CCC morphology and motility.

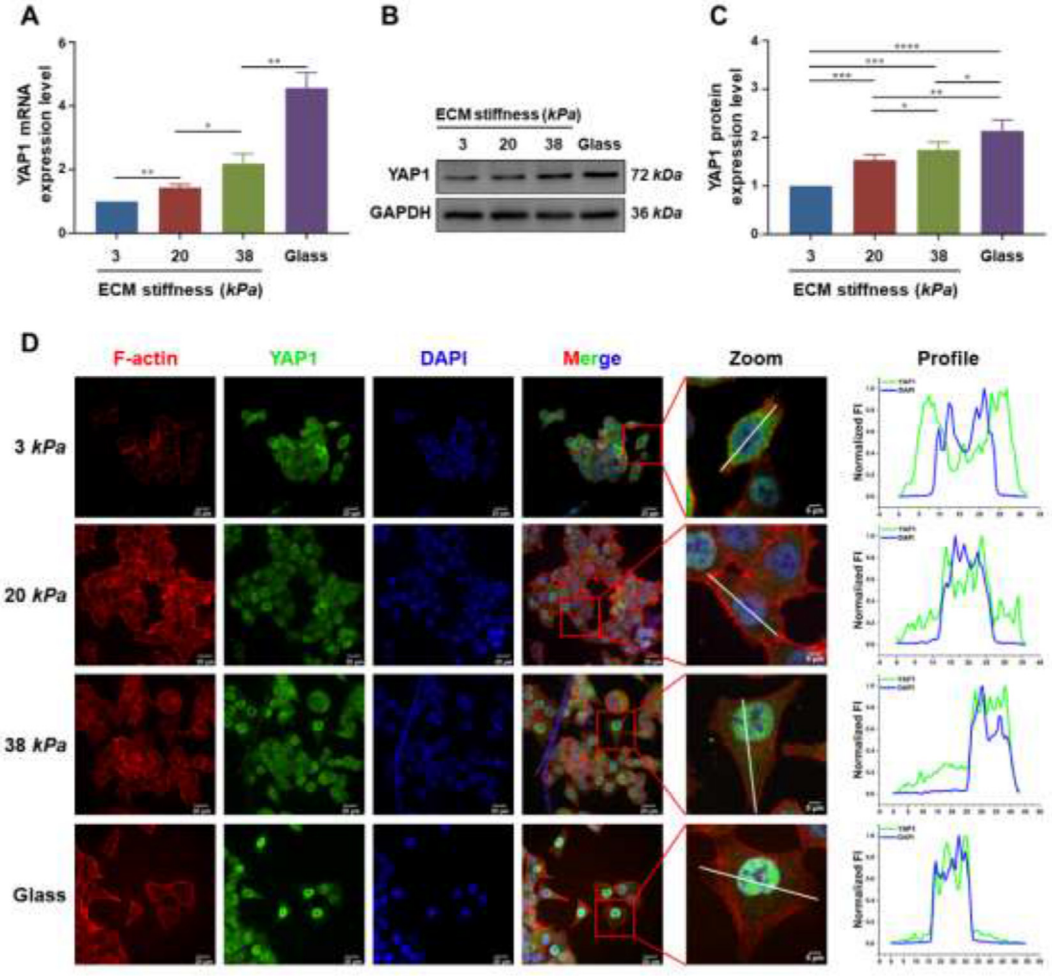

Fig. 6. ECM stiffness promoted the expression and nuclear localization of YAP1. (A) The mRNA expression levels of YAP1 were detected by qRT-PCR on hydrogels of different stiffness. (B, C) The protein expression levels of YAP1 on hydrogels of different stiffness were detected by western blotting and the relative quantification. (D) Immunofluorescence staining of YAP1 shows localization on hydrogels of different stiffness. CCCs were cultured on hydrogels of different stiffness for 48 h and then immunostained for F-actin (phalloidin, red), YAP1 (anti-YAP1, green) and DNA (DAPI, blue). Scale bar = 20 μm. The right images show magnification of the red-boxed regions. Scale bar = 5 μm. Profiles of DAPI and YAP1 were extracted from left panel using ImageJ software, and a line scan plot showing the distribution of DAPI and YAP1 along the direction of the white lines. (mean ± SD; $*p < 0.05$, $**p < 0.01$, $***p < 0.001$ and $****p < 0.0001$).

3.7. YAP1 knockdown inhibited FA clustering and altered the mechanophenotypes of CCCs

During cell migration, the assembly and disassembly of FAs play crucial roles in coordination, adhesion, and retraction at the back-trailing edge.[37] To investigate the mechanism underlying the function of YAP1 in FAs formation, the correlation between the expression levels of YAP1 and paxillin in colon adenocarcinoma cells was analyzed using the GEPIA database. The results showed a positive correlation between the expression levels of YAP1 and paxillin (Fig. 8B). The immunofluorescence staining results (Fig. 8C) showed that YAP1 knockdown cells significantly reduced the number (Fig. 8D) and size (Fig. 8E) of FAs compared with those of shNC cells, while the higher expression of paxillins was distributed throughout the cytoplasm in shYAP1 cells (Fig. 8F), whereas the lower expression of paxillins along the edge of the nucleus to the cell membrane in shNC cells was recruited for FAs assembly. These results indicated that YAP1 regulates FAs formation at the anterior membrane prominence of CCCs. In addition, YAP1 knockdown led to altered mechanophenotypes of CCCs owing to ECM stiffness, including decreased Young's modulus (Fig. 8G), and membrane fluidity (Fig. 8H).

4. Discussion

Distal metastasis is the primary cause of treatment failure in colon cancer.[38,39] Most studies have focused on the chemical factors that regulate the invasion and metastasis of CCCs, including cytokines, the microbiome, and free radicals.[40] However, the regulatory mechanism of the impact of changes in the physical properties (e.g., stiffness) of the tumor microenvironment, induced by peroxidation of the extracellular matrix by free radicals generated by the vigorous metabolism of tumor cells, on the invasion and metastasis of CCCs is not fully understood. In this study, bioinformatics analysis showed that the higher expression level of YAP1 in colon cancer was significantly associated with invasion, metastasis, and reduced patient survival rates (Fig. 1). Therefore, it could be hypothesized that YAP1 may serve as a molecular target for the clinical treatment of distant metastasis of colon cancer.

To determine the direction of cell migration, cells first acquire a characteristic polarization pattern in response to extracellular signals.[41] As shown in Figs. 2 and 3, the morphologies of CCCs, including the spreading area, circularity, and aspect ratio, were significantly positively correlated with their ECM stiffness, suggesting that CCCs could regulate

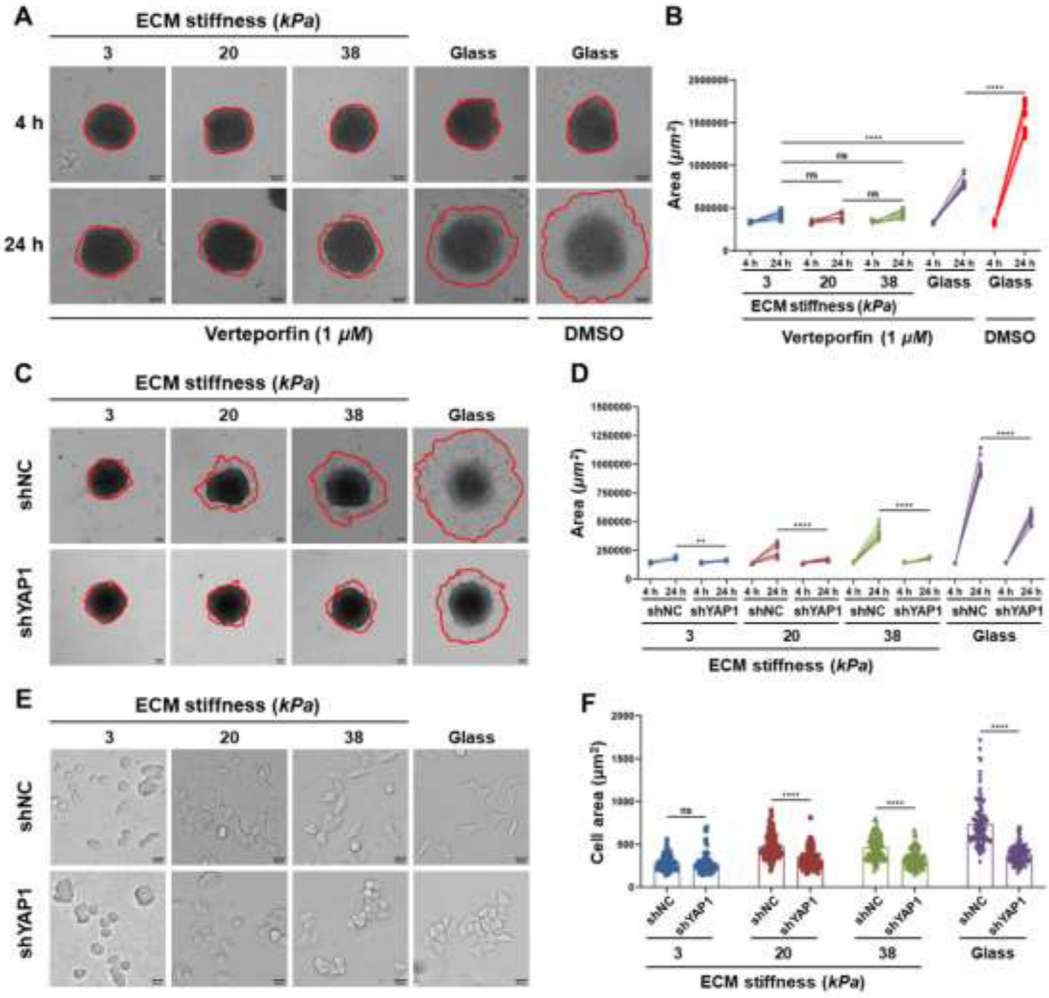

Fig. 7. YAP1 regulated colon cancer metastasis. (A) CCCs multicellular spheroids were transferred to hydrogels of different stiffness (3, 20 and 38 kPa) and Glass, and then treated or untreated with 1 μM verteporfin and allowed to invade for 24 h. Scale bar = 200 μm. (B) The graph depicts the change in area of each spheroid measured at 4 and 24 h by manually outlining spheroids at the indicated time points and calculating the area using ImageJ. (C) The shNC and shYAP1 CCCs multicellular spheroids were cultured on hydrogels with rigidities of 3 kPa, 20 kPa, 38 kPa and Glass, and allowed to invade for 24 h. Scale bar = 200 μm. (D) The graph depicts the change in area of each spheroid measured at 4 and 24 h by manually outlining spheroids at the indicated time points and calculating the area using Image J. (E) Representative phase-contrast images of shNC and shYAP1 CCCs cultured on hydrogels of different stiffnesses for 48 h, and then cell morphology was observed by an inverted microscope. Scale bar = 20 μm. (F) The Cell spreading area of shNC and shYAP1 CCCs were analyzed using ImageJ software. (mean ± SD; ns $p > 0.05$ and ****$p < 0.0001$).

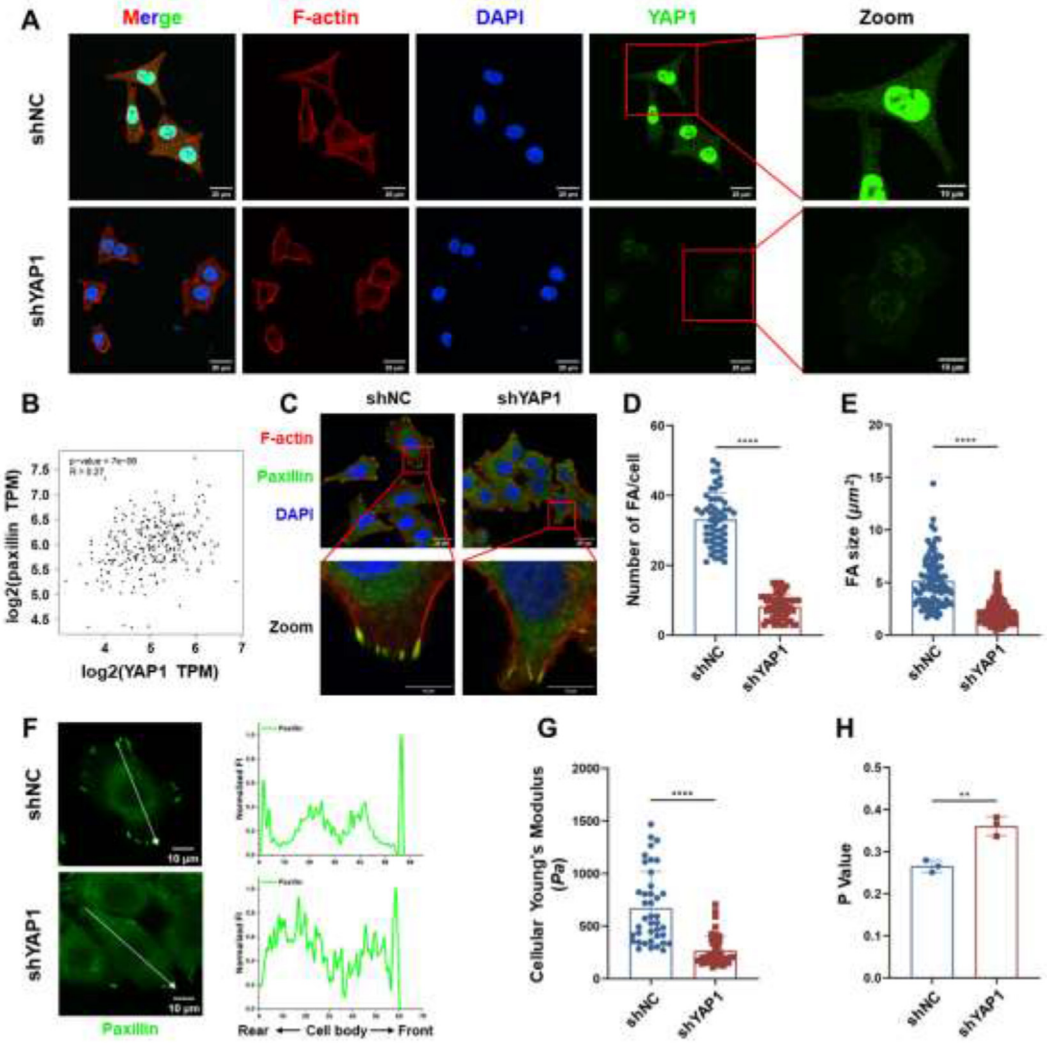

Fig. 8. YAP1 regulated focal adhesion clustering and cellular biomechanical properties of CCCs. (A) Immunofluorescence staining analysis of YAP1 in shNC and shYAP1 CCCs. Cells were cultured on collagen I-coated coverslips for 48 h and then immunostained for F-actin (phalloidin, red), YAP1 (anti-YAP1, green) and DNA (DAPI, blue). Scale bar = 20 μm. The right images show magnification of the red-boxed regions. Scale bar = 10 μm. (B) The correlation between YAP1 and paxillin was analyzed in colon adenocarcinoma patients based on data from the GEPIA2 database. (C) Knockdown of YAP1 expression inhibited focal adhesions in CCCs, cells were fixed and stained for paxillin as a marker for FAs. Scale bar = 20 μm. (D, E) Immunofluorescence images were analyzed for shNC and shYAP1 CCCs to determine number of FA/cells (D) and FA size (E). (F) Left: Cells were inoculated on collagen I-coated coverslips for 48 h, and then immunostained for F-actin (phalloidin, red), paxillin (anti-paxillin, green) and DNA (DAPI, blue). Scale bar = 10 μm. Right: The intensity distribution of paxillin (green) along the direction of the white arrowhead was shown in the line scan plot. (G) Young's modulus of shNC and shYAP1 CCCs was measured from AFM measurement. (H) The fluorescence polarization parameter of shNC and shYAP1 CCCs was quantified. (mean ± SD; $^{**}p < 0.01$ and $^{****}p < 0.0001$).

their shapes in terms of changes in ECM stiffness, which is consistent with previous reports that ECM stiffness affects cell morphology.[42,43] Interestingly, CCCs cultured on a stiffer ECM exhibited a highly polarized morphology compared to those cultured on a soft ECM.

The mechanophenotypes (biomechanical characteristics) of cells change with the physical and chemical extracellular microenvironments, reflecting the relationship between their structure and function.[44] The Young's modulus of cells is an important mechanical characteristic that reflects their stiffness.[45] As shown in Fig. 4D-G, the Young's modulus of CCCs increased with ECM stiffness enhancement, which might be mainly due to the resistance of CCCs to increased ECM-derived mechanical forces to maintain their stable morphology, which is consistent with other recent studies on cervical cancer cells.[42] Second, several studies have found that the invasion and metastasis potential of cancer cells is closely related to EPM; the higher the EPM, the stronger the invasion and metastasis capabilities of the cells.[46] The EPMs of CCCs were enhanced by a stiffer ECM (Fig. 4H), indicating more negative charges of CCCs and more repulsion force between cells, thus promoting the invasion and metastasis of cancer cells. Third, the fluidity of cell membranes is a necessary condition for maintaining physiological functions such as migration, reflecting the dynamic changes in lipid molecules in the plasma membrane,[47] which is associated with the invasion and metastasis of cancer cells.[48,49] As shown in Fig. 4I, the membrane fluidity of CCCs increased significantly with increasing matrix stiffness, which is beneficial for the invasion and metastasis of cancer cells. Based on the above results, alterations in ECM stiffness alter the mechanophenotypes of CCCs, resulting in invasive phenotypes.

Dupont et al. studied the relationship between the YAP1 transcription factor and ECM stiffness and found that YAP1 is a sensor of ECM stiffness-derived mechanical force from the cellular microenvironment.[28] YAP1 regulates the expression of target genes with a wide range of functional effects in many cell and tissue types. The YAP1 signaling pathway is critical for maintaining cellular functions and normal tissue homeostasis, and an imbalance or failure in this process is involved in the occurrence and development of various diseases.[34] Here, polyacrylamide hydrogels with different stiffnesses were used to

simulate normal colon tissue and abnormal colon cancer tissue to further investigate the effect of ECM stiffness colon cancer tissue on CCCs' metastasis via the YAP1 signaling pathway. It has been shown that the colocalization of mechanical sensors at FAs sites enables mechanical and biochemical coupling, leading to sensitivity to changes in extracellular mechanical microenvironments.[16] During migration, cells undergo polarization and form protrusions at the front, where new FAs are formed at protrusion sites. FAs assembly plays a critical role in directed cell migration, and the formation of FAs at the leading edge provides traction against the generation of tensional forces that promote cell migration.[37] As shown in Figs. 5 and 6, the stiffer ECM promoted the formation and maturation of FAs and upregulated the expression levels of paxillins at the membrane protrusion of cells. Furthermore, as crucial molecules for FAs assembly and disassembly, the paxillins mainly colocalized with FAs at the front protrusion of cells along with the increase in ECM stiffness, inferring that the colocalization of FAs and paxillins at the front protrusion of CCCs could be the upstream signal of YAP1. The expression levels and localization of YAP1 in CCCs cultured on different ECM stiffnesses were measured, as shown in Fig. 7; the expression levels of YAP1 in CCCs were markedly upregulated by stiffer ECM, whose localization translocated from the cytoplasm to the nucleus, indicating that YAP1 worked for the changes in ECM stiffness. After inhibiting and silencing YAP1 (Fig. 8), the CCCs showed reduced migration behavior and altered mechanophenotypes, indicating that YAP1 plays key roles in the invasion and metastasis of CCCs in a stiffer ECM microenvironment. Breast cancer cells also show a similar phenomenon.[50] It is possible that YAP1 could serve as a clinical therapeutic target for reducing the invasion and metastatic capability of solid cancer ECM, and anti-fibrotic drugs such as pirfenidone, which downregulate ECM stiffness, may serve as potential clinical treatment options for reducing the distant metastasis of solid cancer cells.

5. Conclusion

In this study, we found that higher expression levels of YAP1 were markedly associated with the invasion and metastasis of CCCs and poor prognosis of colon cancer patients, and that ECM stiffness influenced the invasion and metastasis capability and mechanophenotypes of CCCs via the FA-paxillin-YAP1 signaling pathway. It is important to further understand the invasion and metastasis mechanisms of CCCs, which have laid the theoretical foundation for proposing new clinical protocols for colon cancer from the perspectives of mechanobiology and mechanomedicine.

Author contributions

Kaide Xia: Conceptualization, methodology, data curation, investigation, formal analysis, writing, and Original Draft. **Wenhui Hu:** Formal analysis, methodology, and writing the Original Draft. **Yun Wang:** Project administration and resources. **Jin Chen:** Project administration and resources. **Zuquan Hu:** Project administration; funding acquisition; supervision; validation. **Chenyi An:** Methodology and Resources. **Pu Xu:** Investigation and methodology. **Lijing Teng:** Investigation, methodology, and resources. **Jieheng Wu:** Investigation; methodology. **Lina Liu:** Investigation and resources. **Sichao Zhang:** Methodology and resources. **Jinhua Long:** Project administration, supervision, validation, writing, reviewing, and editing. **Zhu Zeng:** Project administration, conceptualization of resources, supervision, funding acquisition, writing, Review & Editing.

Ethical approval

The CCCs (HCT116) were donated by the Institute of Oncology, Affiliated Tumor Hospital of Guangzhou Medical University (Guangzhou, China). The protocol was approved by the Human and Animal Ethics Committee of Guizhou Medical University (No. 2023-46).

Declaration of competing interest

The authors declare that they have no known competing financial interests or personal relationships that could have appeared to influence the work reported in this paper.

Acknowledgement

This study was supported by the National Natural Science Foundation of China (grant numbers 12132006, 32371373, 31771014, and 82060555).

Appendix A. Supplementary data

Supplementary data to this article can be found online at https://doi.org/10.1016/j.mbm.2024.100062.

References

1. Sung H, Ferlay J, Siegel RL, et al. Global cancer statistics 2020: GLOBOCAN estimates of incidence and mortality worldwide for 36 cancers in 185 countries. *CA Cancer J Clin*. 2021;71(3):209–249. https://doi.org/10.3322/caac.21660.
2. Siegel RL, Miller KD, Wagle NS, Jemal A. Cancer statistics, 2023. *CA Cancer J Clin*. 2023;73(1):17–48. https://doi.org/10.3322/caac.21763.
3. Chandra R, Karalis JD, Liu C, et al. The colorectal cancer tumor microenvironment and its impact on liver and lung metastasis. *Cancers (Basel)*. 2021;13(24):6206. https://doi.org/10.3390/cancers13246206, 6206.
4. Heinz MC, Peters NA, Oost KC, et al. Liver colonization by colorectal cancer Metastases requires YAP-controlled plasticity at the micrometastatic stage. *Cancer Res*. 2022;82(10):1953–1968. https://doi.org/10.1158/0008-5472.CAN-21-0933.
5. Liu G, Zhang Y, Huang Y, Yuan X, Cao Z, Zhao Z. PTPN6-EGFR protein complex: a novel target for colon cancer metastasis. *J Oncol*. 2022;2022:7391069. https://doi.org/10.1155/2022/7391069.
6. Siegel RL, Miller KD, Fedewa SA, et al. Colorectal cancer statistics, 2017. *CA Cancer J Clin*. 2017;67(3):177–193. https://doi.org/10.3322/caac.21395.
7. Yuan Y, Jiang YC, Sun CK, Chen QM. Role of the tumor microenvironment in tumor progression and the clinical applications. *Oncol Rep*. 2016;35(5):2499–2515. https://doi.org/10.3892/or.2016.4660.
8. Ren B, Cui M, Yang G, et al. Tumor microenvironment participates in metastasis of pancreatic cancer. *Mol Cancer*. 2018;17(1):108. https://doi.org/10.1186/s12943-018-0858-1.
9. Ladoux B, Mege RM. Mechanobiology of collective cell behaviours. *Nat Rev Mol Cell Biol*. 2017;18(12):743–757. https://doi.org/10.1038/nrm.2017.98.
10. Li X, Wang J. Mechanical tumor microenvironment and transduction: cytoskeleton mediates cancer cell invasion and metastasis. *Int J Biol Sci*. 2020;16(12):2014–2028. https://doi.org/10.7150/ijbs.44943.
11. Eble JA, Niland S. The extracellular matrix in tumor progression and meta-stasis. *Clin Exp Metastasis*. 2019;36(3):171–198. https://doi.org/10.1007/s10585-019-09966-1.
12. Pickup MW, Mouw JK, Weaver VM. The extracellular matrix modulates the hallmarks of cancer. *EMBO Rep*. 2014;15(12):1243–1253. https://doi.org/10.15252/embr.201439246.
13. Kanchanawong P, Calderwood DA. Organization, dynamics and mechanoregulation of integrin-mediated cell-ECM adhesions. *Nat Rev Mol Cell Biol*. 2023;24(2):142–161. https://doi.org/10.1038/s41580-022-00531-5.
14. Seong J, Wang N, Wang Y. Mechanotransduction at focal adhesions: from physiology to cancer development. *J Cell Mol Med*. 2013;17(5):597–604. https://doi.org/10.1111/jcmm.12045.
15. Tan F, Huang Y, Pei Q, Liu H, Pei H, Zhu H. Matrix stiffness mediates stemness characteristics via activating the Yes-associated protein in colorectal cancer cells. *J Cell Biochem*. 2018:2213–2225. https://doi.org/10.1002/jcb.27532.
16. Grudtsyna V, Packirisamy S, Bidone TC, Swaminathan V. Extracellular mat-rix sensing via modulation of orientational order of integrins and F-actin infocal adhesions. *Life Sci Alliance*. 2023;6(10):e202301898. https://doi.org/10.26508/lsa.202301898.
17. Piersma B, Hayward MK, Weaver VM. Fibrosis and cancer: a strained rel-ationship. *Biochim Biophys Acta Rev Cancer*. 2020;1873(2):188356. https://doi.org/10.1016/j.bbcan.2020.188356.
18. Paluch EK, Aspalter IM, Sixt M. Focal adhesion-independent cell migration. *Annu Rev Cell Dev Biol*. 2016;32:469–490. https://doi.org/10.1146/annurev-cellbio-111315-125341.
19. Chandrashekar DS, Bashel B, Balasubramanya SAH, et al. UALCAN: a portal for facilitating tumor subgroup gene expression and survival analyses. *Neoplasia*. 2017;19(8):649–658. https://doi.org/10.1016/j.neo.2017.05.002.
20. Tang Z, Li C, Kang B, Gao G, Li C, Zhang Z. GEPIA: a web server for cancer and normal gene expression profiling and interactive analyses. *Nucleic Acids Res*. 2017;45(W1):W98–W102. https://doi.org/10.1093/nar/gkx247.
21. Tse JR, Engler AJ. Preparation of hydrogel substrates with tunable mechanical properties. *Curr Protoc Cell Biol. Chapter*. 2010;10. https://doi.org/10.1002/0471143030.cb1016s47. Unit 10 16.

22. Peng Y, Chen Z, Chen Y, et al. ROCK isoforms differentially modulate cancer cell motility by mechanosensing the substrate stiffness. *Acta Biomater*. 2019;88:86–101. https://doi.org/10.1016/j.actbio.2019.02.015.
23. Syed S, Schober J, Blanco A, Zustiak SP. Morphological adaptations in breast cancer cells as a function of prolonged passaging on compliant substrates. *PLoS One*. 2017; 12(11):e0187853. https://doi.org/10.1371/journal.pone.0187853.
24. McKenzie AJ, Hicks SR, Svec KV, Naughton H, Edmunds ZL, Howe AK. The mechanical microenvironment regulates ovarian cancer cell morphology, migration, and spheroid disaggregation. *Sci Rep*. 2018;8(1):7228. https://doi.org/10.1038/s41598-018-25589-0.
25. Feng F, Feng X, Zhang D, Li Q, Yao L. Matrix stiffness induces pericyte-fibroblast transition through YAP activation. *Front Pharmacol*. 2021;12:698275. https://doi.org/10.3389/fphar.2021.698275.
26. Gorelik R, Gautreau A. Quantitative and unbiased analysis of directional pe-rsistence in cell migration. *Nat Protoc*. 2014;9(8):1931–1943. https://doi.org/10.1038/nprot.2014.131.
27. Hu ZQ, Xue H, Long JH, et al. Biophysical properties and motility of human mature dendritic cells deteriorated by vascular endothelial growth factor through cytoskeleton remodeling. *Int J Mol Sci*. 2016;17(11):1756. https://doi.org/10.3390/ijms17111756.
28. Dupont S, Morsut L, Aragona M, et al. Role of YAP/TAZ in mechanotransduction. *Nature*. 2011;474(7350):179–183. https://doi.org/10.1038/nature10137.
29. Cai X, Wang KC, Meng Z. Mechanoregulation of YAP and TAZ in cellular homeostasis and disease progression. *Front Cell Dev Biol*. 2021;9:673599. https://doi.org/10.3389/fcell.2021.673599.
30. Despotovic SZ, Milicevic NM, Milosevic DP, et al. Remodeling of extracellular matrix of the lamina propria in the uninvolved human rectal mucosa 10 and 20 cm away from the malignant tumor. *Tumour Biol*. 2017;39(7):1010428317711654. https://doi.org/10.1177/1010428317711654.
31. Wei B, Zhou X, Liang C, et al. Human colorectal cancer progression correlates with LOX-induced ECM stiffening. *Int J Biol Sci*. 2017;13(11):1450–1457. https://doi.org/10.7150/ijbs.21230.
32. Nebuloni M, Albarello L, Andolfo A, et al. Insight on colorectal carcinoma infiltration by studying perilesional extracellular matrix. *Sci Rep*. 2016;6:22522. https://doi.org/10.1038/srep22522.
33. Johnson LA, Rodansky ES, Sauder KL, et al. Matrix stiffness corresponding to strictured bowel induces a fibrogenic response in human colonic fibroblasts. *Inflamm Bowel Dis*. 2013;19(5):891–903. https://doi.org/10.1097/MIB.0b013e3182813297.
34. Kawano S, Kojima M, Higuchi Y, et al. Assessment of elasticity of colorectal cancer tissue, clinical utility, pathological and phenotypical relevance. *Cancer Sci*. 2015; 106(9):1232–1239. https://doi.org/10.1111/cas.12720.
35. Seetharaman S, Etienne-Manneville S. Cytoskeletal crosstalk in cell migration. *Trends Cell Biol*. 2020;30(9):720–735. https://doi.org/10.1016/j.tcb.2020.06.004.
36. Broussard JA, Webb DJ, Kaverina I. Asymmetric focal adhesion disassembly in motile cells. *Curr Opin Cell Biol*. 2008;20(1):85–90. https://doi.org/10.1016/j.ceb.2007.10.009.
37. Ridley AJ, Schwartz MA, Burridge K, et al. Cell migration: integrating signals from front to back. *Science*. 2003;302(5651):1704–1709. https://doi.org/10.1126/science.1092053.
38. Chen Y, Chen Y, Zhang J, et al. Fusobacterium nucleatum promotes metastasis in colorectal cancer by activating autophagy signaling via the upregulation of CARD3 expression. *Theranostics*. 2020;10(1):323–339. https://doi.org/10.7150/thno.38870.
39. Zhang YF, Li CS, Zhou Y, Lu XH. Effects of propofol on colon cancer metastasis through STAT3/HOTAIR axis by activating WIF-1 and suppressing Wnt pathway. *Cancer Med*. 2020;9(5):1842–1854. https://doi.org/10.1002/cam4.2840.
40. Underwood PW, Ruff SM, Pawlik TM. Update on targeted therapy and immunotherapy for metastatic colorectal cancer. *Cells*. 2024;13(3):245. https://doi.org/10.3390/cells13030245.
41. Ladoux B, Mege RM, Trepat X. Front-rear polarization by mechanical cues: from single cells to tissues. *Trends Cell Biol*. 2016;26(6):420–433. https://doi.org/10.1016/j.tcb.2016.02.002.
42. Zhuang Y, Huang Y, He Z, Liu T, Yu X, Xin SX. Effect of substrate stiffness on the mechanical properties of cervical cancer cells. *Arch Biochem Biophys*. 2022;725: 109281. https://doi.org/10.1016/j.abb.2022.109281.
43. Asano S, Ito S, Takahashi K, et al. Matrix stiffness regulates migration of human lung fibroblasts. *Phys Rep*. 2017;5(9):e13281. https://doi.org/10.14814/phy2.13281.
44. Zeng Z, Xu X, Chen D. Dendritic cells: biophysics, tumor microenvironment and Chinese traditional medicine. *SpringerBriefs Biochem Mol Biol*. 2015;1:1–66. https://doi.org/10.1007/978-94-017-7405-5.
45. Xia T, Zhao R, Liu W, et al. Effect of substrate stiffness on hepatocyte migration and cellular Young's modulus. *J Cell Physiol*. 2018;233(9):6996–7006. https://doi.org/10.1002/jcp.26491.
46. Li Z, Li Y, Wang N, Yang L, Zhao W, Zeng X. Establishment and analysis of osteosarcoma cell sublines with different metastatic characteristics. *Tumour Biol*. 2014;35(9):8591–8596. https://doi.org/10.1007/s13277-014-2029-3.
47. Zeng Z, Liu X, Jiang Y, et al. Biophysical studies on the differentiation of human CD14+ monocytes into dendritic cells. *Cell Biochem Biophys*. 2006;45(1):19–30. https://doi.org/10.1385/CBB:45:1:19.
48. Ajdzanovic V, Mojic M, Maksimovic-Ivanic D, et al. Membrane fluidity, invasiveness and dynamic phenotype of metastatic prostate cancer cells after treatment with soy isoflavones. *J Membr Biol*. 2013;246(4):307–314. https://doi.org/10.1007/s00232-013-9531-1.
49. Zhao W, Prijic S, Urban BC, et al. Candidate antimetastasis drugs suppress the metastatic capacity of breast cancer cells by reducing membrane fluidity. *Cancer Res*. 2016;76(7):2037–2049. https://doi.org/10.1158/0008-5472.CAN-15-1970.
50. Shen J, Cao B, Wang Y, et al. Hippo component YAP promotes focal adhesion and tumour aggressiveness via transcriptionally activating THBS1/FAK signalling in breast cancer. *J Exp Clin Cancer Res*. 2018;37(1):175. https://doi.org/10.1186/s13046-018-0850-z.